ACS NANO
Cite This: ACS Nano 2018, 12, 11062−11069
www.acsnano.org

ARTICLE

Highly Reliable Superhydrophobic Protection for Organic Field-Effect Transistors by Fluoroalkylsilane-Coated TiO_2 Nanoparticles

Daekyoung Yoo,[†] Youngrok Kim,[†] Misook Min,[†,∥] Geun Ho Ahn,[‡] Der-Hsien Lien,[‡] Jingon Jang,[†] Hyunhak Jeong,[†] Younggul Song,[†] Seungjun Chung,[*,§] Ali Javey,[‡] and Takhee Lee[*,†]

[†]Department of Physics and Astronomy, and Institute of Applied Physics, Seoul National University, Seoul 08826, Korea
[‡]Electrical Engineering and Computer Sciences, University of California, Berkeley, California 94720, United States
[§]Photo-Electronic Hybrids Research Center, Korea Institute of Science and Technology, Seoul 02792, Korea

Supporting Information

ABSTRACT: One of the long-standing problems in the field of organic electronics is their instability in an open environment, especially their poor water resistance. For the reliable operation of organic devices, introducing an effective protection layer using organo-compatible materials and processes is highly desirable. Here, we report a facile method for the depositing of an organo-compatible superhydrophobic protection layer on organic semiconductors under ambient conditions. The protection layer exhibiting excellent water-repellent and self-cleaning properties was deposited onto organic semiconductors directly using a dip-coating process in a highly fluorinated solution with fluoroalkylsilane-coated titanium dioxide (TiO_2) nanoparticles. The proposed protection layer did not damage the underlying organic semiconductors and had good resistance against mechanical-, thermal-, light-stress-, and water-based threats. The protected organic field-effect transistors exhibited more-reliable electrical properties, even when exposed to strong solvents, due to its superhydrophobicity. This study provides a practical solution with which to enhance the reliability of environmentally sensitive organic semiconductor devices in the natural environment.

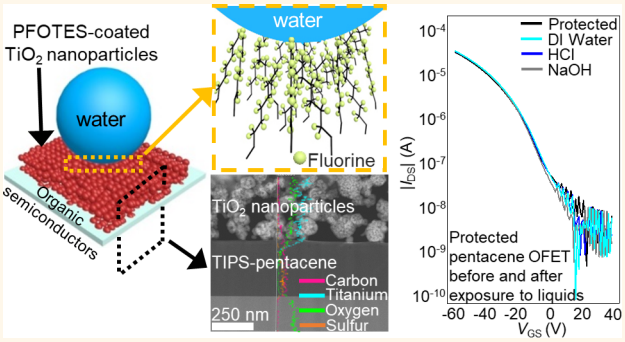

KEYWORDS: *superhydrophobic surface, organic semiconductor, nanoparticles, reliability, organic electronics*

Organic semiconductors have attracted significant interest for electronic device applications with low-cost and low-temperature processabilities.[1−7] They can also be regarded as one of the promising candidates to be employed in additive manufacturing such as printing processes.[8−11] Nevertheless, it is widely reported that they suffer from environmental instability; in particular, they can be drastically degraded by water-based hindrances.[12−15] Although many efforts to address this issue by encapsulating with various materials such as parylene, silicone, barrier foil, or a superhydrophobic glass have been reported,[13,16−19] studies on organo-compatible materials and processing to introduce an effective protection layer that can be directly deposited onto organic components are highly desirable. In this regard, the introduction of a superhydrophobic protection layer onto organic semiconductors can be a promising approach to realizing more-reliable organic semiconductor applications because superhydrophobic protection layers provide the attractive water repellency, which could eliminate water-based hindrances from surfaces of organic semiconductors. The materials and processes for the superhydrophobic protection layer formation need to be organo-compatible so that they do not damage physically or chemically when placed on the organic layers, and thus, their electrical characteristics would not be degraded. In addition, fast, facile, and low-cost approaches to implementing the protection layer are desirable for providing the advantages of organic components.

In this study, we report an organo-compatible superhydrophobic protection layer that can be directly deposited onto various organic semiconductors for highly reliable organic field-effect transistors (OFETs). The protection layer could be introduced by simply dipping OFETs into a highly fluorinated solvent with fluoroalkylsilane-coated TiO_2 nanoparticles. By

Received: July 11, 2018
Accepted: October 10, 2018
Published: October 10, 2018

DOI: 10.1021/acsnano.8b05224
ACS Nano 2018, 12, 11062−11069

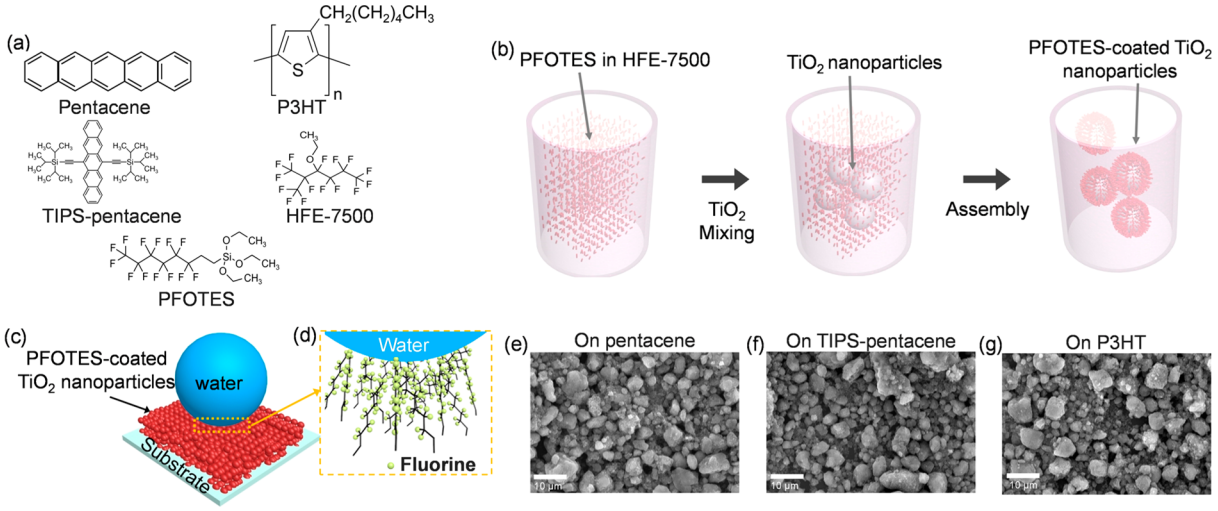

Figure 1. (a) Molecular structures of pentacene, TIPS-pentacene, P3HT, HFE-7500, and PFOTES. (b) Schematic for preparing the solution of PFOTES-coated TiO_2 nanoparticles. (c) Schematic of a water droplet contacting the PFOTES-coated TiO_2 nanoparticle layers on organic semiconducting layers. (d) Schematic for the interface between water and the fluorinated end-groups of PFOTES. (e–g) SEM images for the PFOTES-coated TiO_2 nanoparticles on (e) pentacene, (f) TIPS-pentacene, and (g) P3HT layers.

optimizing the solvent system and taking surface energy into consideration, the uniform protection layer could be deposited onto universal organic semiconductors without any physical damage. The surface roughness of a TiO_2 nanoparticle-based protection layer allowed for excellent water repellence and self-cleaning abilities regardless of underlying organic semiconductors. The presented superhydrophobic protection layer provided the much-improved stability of OFETs against water-based threats and ambient air while exhibiting good resistance against thermal and mechanical stresses. Therefore, this method can foster more-reliable organic electronics working in an outdoor environment.

RESULTS AND DISCUSSION

A solution process using 1*H*,1*H*,2*H*,2*H*-perfluorooctyltriethoxysilane (PFOTES) attached to TiO_2 nanoparticles (average diameter of <100 nm) dispersed in 3-ethoxy-1,1,1,2,3,4,4,5,5,6,6,6-dodecafluoro-2-trifluoromethylhexane (HFE-7500) was conducted to form the protection layer (Figure 1a). Highly fluorinated HFE-7500 is immiscible to most organic materials; thus, the solution-dipping process does not damage organic layer during the protection layer formation.[20] Moreover, PFOTES has been widely used to introduce superhydrophobic properties on the surface of TiO_2 nanoparticles by reacting with hydroxyl groups (Figure 1b).[21−23] Therefore, PFOTES-coated TiO_2 nanoparticle layers can deliver superhydrophobic properties to protect the underlying organic layer from water-based solutions without additional surface treatments, structures, or dedicated procedures (Figure 1c,d). Note that the PFOTES-coated TiO_2 nanoparticles highly dispersed in HFE-7500 (14.0 wt %) allow excellent film formation universally on various organic semiconductors [pentacene, 6,13-bis(triisopropylsilylethynyl)-pentacene (TIPS-pentacene), and poly(3-hexylthiophene (P3HT) for thermally evaporated organic small-molecule, solution-deposited organic small-molecule, and solution-deposited polymer semiconductors, respectively] by simply dipping them into the prepared solution for a short time (~2 s) in ambient conditions (see Figure S1 and Table S1 for a detailed description). It should be noted that this simple dipping process was enough to produce the uniformly deposited TiO_2 nanoparticle layers because the solution had excellent dispersion ability and wetting properties onto all of the semiconductors used in this study as well as on the Au contacts and SiO_2 gate dielectric (see Figures S2–S4). As a result, the protection layers having similar morphologies were produced onto all of the different organic semiconductors (Figure 1e–g). In addition, the surface coverages after coating with different TiO_2 nanoparticle densities were also studied (see Figure S5). The surface roughness of the PFOTES-coated TiO_2 nanoparticle layers was measured using a 3-dimensional (3D) laser profiler and atomic force microscope (AFM) (see Figures S6 and S7). The surface roughness of TiO_2 nanoparticles and the low surface energy induced by the trifluoromethyl ($-CF_3$) groups[24] of PFOTES make up the superhydrophobic surface,[25] which delivered a high contact angle of >150° regardless of the underlying organic semiconducting layers (Figure 2a), whereas the bare pentacene layer exhibited a water-contact angle of 81° (Figure 2b). Also, the low contact-angle hysteresis (<5°) was observed for liquids having surface tension values over 44 mN m^{-1} (see Figure S8). It is well-known that high contact angles and low contact-angle hysteresis can be observed in micro- and nanoscale hierarchical superhydrophobic surfaces because of air gaps in roughened surfaces that play a critical role for water repellency of superhydrophobic surfaces (see Figure S9).[25−28] Therefore, our surface morphology produced by the simple dipping process with PFOTES-coated TiO_2 nanoparticles created enough air gaps to allow extreme water repellency, showing the ability of water bouncing comparable with other reported superhydrophobic surfaces (Figure 2c).[19,22,23,25−31] For further investigation, various liquid droplets having different surface tensions were also dropped with various speeds ranging from 0.3 to 1.7 m s^{-1} onto the surface of the protection layer. Even liquid droplets having surface tension values of >44 mN m^{-1} were easily bounced off from the surface of our superhydrophobic protection layer as a whole or fragmented droplets (see Table S2 and Figure S10). In addition, an extremely small roll-off angle (<1°) was observed for the deposited PFOTES-coated TiO_2 nanoparticle layers, whereas

DOI: 10.1021/acsnano.8b05224
ACS Nano 2018, 12, 11062−11069

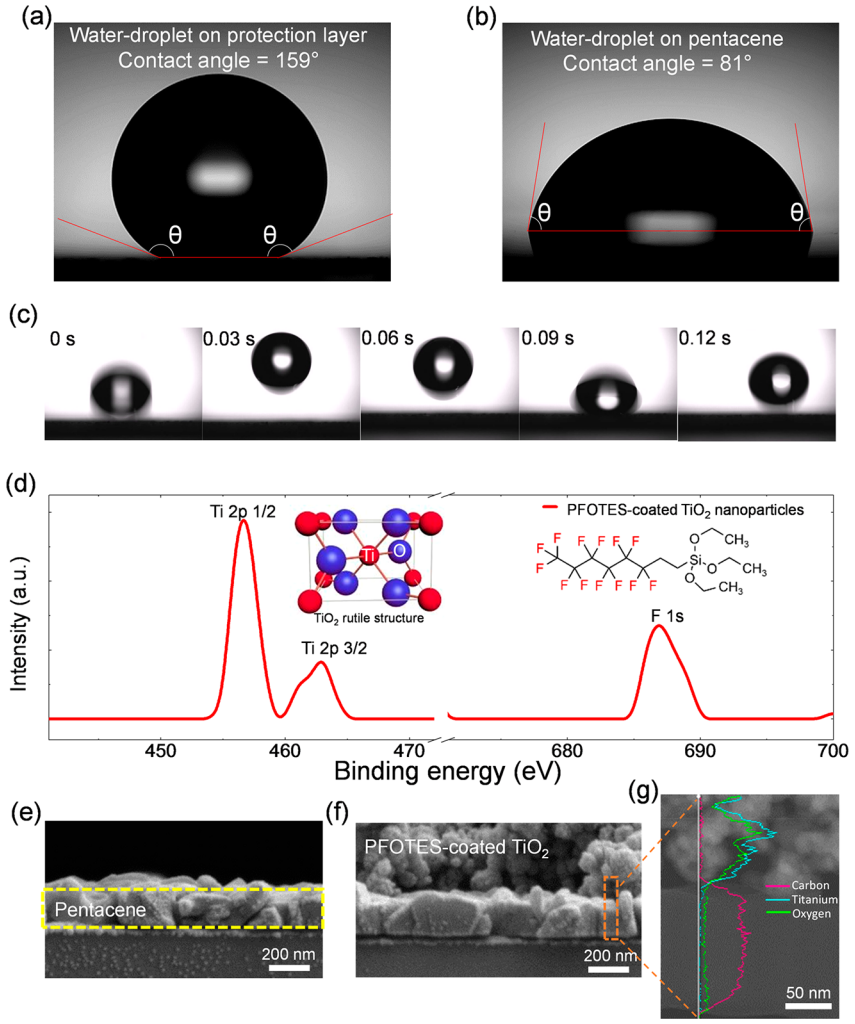

Figure 2. (a) Optical image of the water contact angle on a protected pentacene layer with the PFOTES-coated TiO_2 nanoparticles. (b) Optical image of the water-contact angle on a bare pentacene layer. (c) Time-resolved images for water droplet bouncing on the PFOTES-coated TiO_2 nanoparticle layers. (d) X-ray spectroscopy analysis of PFOTES-coated TiO_2 nanoparticle layers. The inset image shows the rutile phase of TiO_2 and the molecular structure of PFOTES with the fluorine atoms highlighted in red. (e, f) SEM images of the pentacene layers (e) without and (f) with the PFOTES-coated TiO_2 nanoparticle layers. (g) TEM image and energy-dispersive X-ray spectroscopy data of the PFOTES-coated TiO_2 nanoparticle layers on a pentacene layer.

relatively large roll-off angle of 34° was observed for the bare pentacene (see Figure S11). The small roll-off angle of the PFOTES-coated TiO_2 nanoparticle layers allows the self-cleaning ability upon exposure to water-based solvents. In other words, undesirable substances, even heavy soils, were successfully swept away by continuously dropping water droplets because the sliding water droplets picked up the soils from the surface of the self-cleaning layer (see Figure S12). The presented water-bouncing and self-cleaning abilities from the roughened surface of the PFOTES-coated nanoparticles could offer superhydrophobic protection for OFETs, which is useful for realizing more practical applications.

To examine the proposed superhydrophobic protection layer, X-ray photoelectron spectroscopy (XPS) was conducted on the TiO_2 nanoparticle films with and without the PFOTES layer coated by the aforementioned facile dipping process. The XPS spectrum showed intense photoelectron signals on the surface at binding energies of 457 and 463 eV related to the Ti $2p_{1/2}$ and $2p_{3/2}$ levels of the titanium atoms, respectively.[22,32] The F 1s peak was clearly observed at the binding energy of 687 eV on the PFOTES-coated TiO_2 nanoparticle film (Figure 2d), whereas the TiO_2 nanoparticle film without PFOTES showed the absence of fluorine atoms (see Figure S13).[22] Because no clear peak related to the F 1s orbital was observed in the TiO_2 nanoparticle film without PFOTES, the fluorine contained in HFE-7500 did not remain on the surface of the TiO_2 nanoparticles after the drying process. Note that the TiO_2 nanoparticle layers without PFOTES did not exhibit superhydrophobicity at all, which indicates that PFOTES plays a critical role in achieving low-surface energy (see Figure S14).

To confirm that the methods and materials used in this work are organo-compatible, cross-sectional images of the organic semiconducting layers with and without the PFOTES-coated TiO_2 nanoparticle layers were obtained. Scanning electron microscopy (SEM) images revealed that the PFOTES-coated TiO_2 nanoparticle layers were well-deposited on the pentacene semiconducting layer, and they did not produce any physical damages to the pentacene layer (Figure 2e,f). Moreover, the cross-sectional transmission electron microscope (TEM) and energy-dispersive X-ray spectroscopy (EDS) results also indicated that no undesirable penetration was observed after the superhydrophobic protection layer deposition because the

DOI: 10.1021/acsnano.8b05224
ACS Nano 2018, 12, 11062−11069

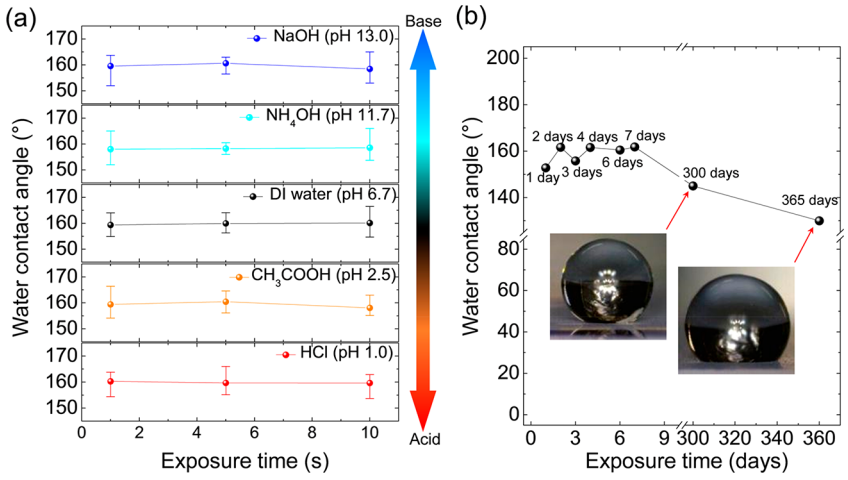

Figure 3. (a) Water-contact angles of the superhydrophobic layer after exposure to HCl (pH 1.0), CH_3COOH (pH 2.5), DI water (pH 6.7), NH_4OH (pH 11.7), and NaOH (pH 13.0) droplets for 1, 5, and 10 s. (b) Water-contact angles of the PFOTES-coated TiO_2 nanoparticle layers after exposure to air for 1 year.

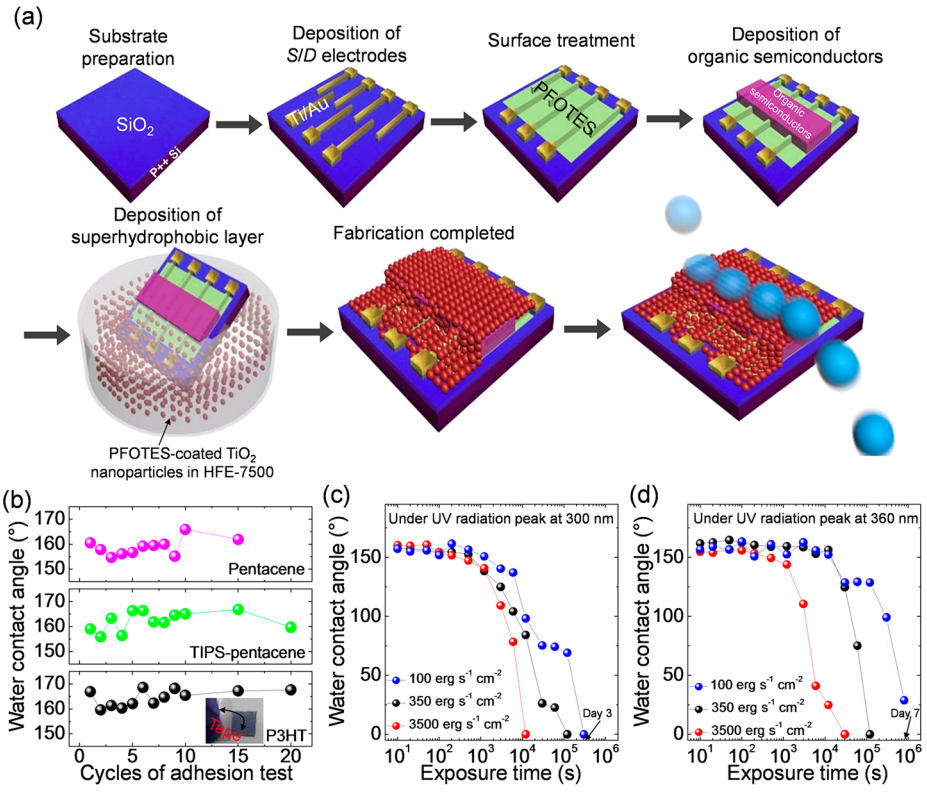

Figure 4. (a) Fabrication process of OFETs with PFOTES-coated TiO_2 nanoparticle layers as a superhydrophobic protection layer. (b) Water-contact angles of the superhydrophobic layer on three organic semiconductors in the adhesion test using commercial cellophane tape. (c, d) Degradation of water-contact angles under UV light exposure with a peak wavelength of (c) 300 and (d) 360 nm for different light powers.

titanium and oxygen elements were evidently detected only in the upper PFOTES-coated TiO_2 nanoparticle layers but were undetected in the underlying pentacene layer (Figure 2g). We also did not observe physical damages and penetration issues on solution-processed TIPS-pentacene and P3HT layers during the protection layer formation (see Figure S15). Therefore, the prepared superhydrophobic protection layer could be universally applicable to various organic electronics without chemically and physically penetrating into underlying sensitive organic semiconductors. In addition to *p*-type organic semiconductors, our superhydrophobic protection layer could be applied to *n*-type organic semiconductors without physical and chemical damage (see Figure S16).

To use organic devices in practical applications, an excellent tolerance to realistic circumstances is necessary to achieve reliable operation that maintains their electrical characteristics when exposed to, for example, water, acid rain (pH < 5.6),[33] various beverages (pH 3.0−6.5),[34] and cleaning soaps (pH 9.0−12.0)[35,36] that can be met in daily life. Therefore, an effective protection layer should have a good robustness

DOI: 10.1021/acsnano.8b05224
ACS Nano 2018, 12, 11062−11069

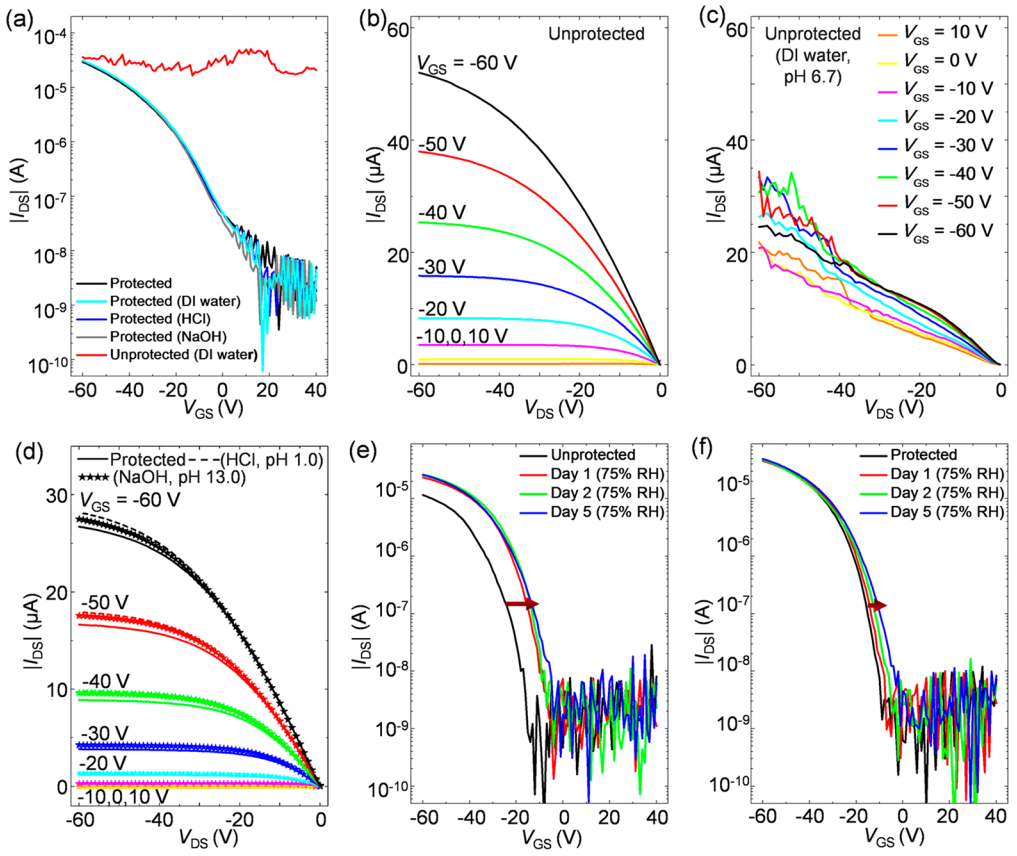

Figure 5. (a) Transfer curves on the semilogarithmic scale for an unprotected pentacene OFET (*i.e.*, without PFOTES-coated TiO_2 nanoparticle layers) after exposure to DI water and for a protected pentacene OFET (*i.e.*, coated with PFOTES-coated TiO_2 nanoparticle layers) before and after exposure to aqueous solutions of different pH ranging from 1 to 13. (b) Output curves for unprotected pentacene OFETs before exposure to DI water. (c) Output curves for unprotected pentacene OFETs after exposure to DI water. (d) Output curves of the protected pentacene OFET with the PFOTES-coated TiO_2 nanoparticle layers before and after exposure to strong acid (HCl) and base (NaOH). (e, f) Transfer curves on the semilogarithmic scale for the (e) unprotected and (f) protected TIPS-pentacene OFETs after exposure to water vapor (75% relative humidity at 20 °C).

against liquid-based substances with a wide range of pH values to prevent operation failure. To confirm the robustness of the protection film, contact angles were measured after exposure to various corrosive liquids, such as hydrochloric acid (HCl, pH 1.0), sodium hydroxide (NaOH, pH 13.0), acetic acid (CH_3COOH, pH 2.7), ammonium hydroxide (NH_3OH, pH 11.7), and deionized (DI) water for 10 s. Even though the prepared protection film was exposed to strong acid and alkaline solvents, its superhydrophobicity was well-maintained exhibiting a contact angle of over 150° (Figure 3a). Detailed information on the robustness of the prepared protection layers to corrosive liquids is presented in Figure S17. Although the superhydrophobicity of the PFOTES-coated TiO_2 nanoparticle layers slightly degraded, showing a contact angle of ~130° due to increased surface energy after exposure to air for 1 year, the PFOTES-coated TiO_2 nanoparticle layers still exhibited sufficient hydrophobicity to prevent water-based threats, which indicates good durability in ambient (Figure 3b). With these attractive benefits, the proposed protection layer was used for environmentally sensitive OFETs (Figure 4a) and the protection layer had good resistance upon mechanical, thermal, and light stress.

We performed an adhesion test with a piece of commercial cellophane tape more than 15 times for the superhydrophobic protection layer on different organic semiconductors. The results showed that the PFOTES-coated TiO_2 nanoparticle layers exhibited good adhesion properties without delamination issues on various organic semiconductors, maintaining their superhydrophobicity with a contact angle over 150° in these durability tests (Figure 4b). Furthermore, under shear pressure by friction between a commercial rubber roller and the prepared PFOTES-coated TiO_2 nanoparticle layers, their superhydrophobicity was well-maintained during the 50 rollings with shearing pressure of 1 kPa and speed of 1 cm s^{-1} (see Figure S18). Importantly, the rough surface, which is a critical factor for introducing superhydrophobicity, was still well-preserved without critical structure collapse under vertical pressure of up to 50 N cm^{-2}, exhibiting an average water contact angle over 150° (see Figure S19). Also, superhydrophobicity of the PFOTES-coated TiO_2 nanoparticle layers under tensile strain was well maintained after 10 000 bending cycles and even at stretching conditions (see Figures S20 and S21). Furthermore, the superhydrophobicity did not degrade against a tap water with dynamic pressure of approximately 100 kPa for 100 s, and its extreme water repellency enable tap water to bounce off of the surface (see Figure S22).

The thermal stability of the PFOTES-coated TiO_2 nanoparticle layers was also evaluated by measuring a water-contact angle after the thermal treatment processes. The water-contact angles of the PFOTES-coated TiO_2 nanoparticle layer were well-maintained when placed onto a 80 °C hot-plate for a day

DOI: 10.1021/acsnano.8b05224
ACS Nano 2018, 12, 11062−11069

(see Figure S23), but its superhydrophobicity was drastically degraded as the annealing temperature was increased up to 250 °C because it is close to the desorption temperature of PFOTES (see Figure S23).[37] However, the stable superhydrophobic property was exhibited at 200 °C, and even the PFOTES-coated TiO_2 nanoparticle layers were kept on a hot plate for 3 h regardless of underlying organic semiconductors (see Figure S23).

A pair of ultraviolet (UV) lamps with a peak wavelength of 300 and 360 nm were used to investigate the changes of superhydrophobicity after exposure to UV light. The following results in Figure 4c,d indicated that the contact angle decreased after exposure to UV light with power of 3500 erg s^{-1} cm^{-2}, corresponding to 0.35 mW cm^{-2} for 10^3 s. The degradation of the contact angle was delayed up to 10^5 s as the UV lamp power was reduced (~100 erg s^{-1} cm^{-2} corresponding to 0.01 mW cm^{-2}). In addition, the degradation of superhydrophobicity after exposing to visible lights was also investigated (see Figure S24). By the exploitation of these behaviors, switchable surface energy of the TiO_2 surfaces is available, exhibiting reversible superhydrophobicity (>150°) and superhydrophilicity (~0°) (see Figure S24).

We systematically performed studies to confirm that our superhydrophobic protection layers produced by the facile, organo-compatible, and universal process could be a good alternative strategy to improving the electrical reliability of OFETs for water-based threats. We characterized the electrical characteristics of various OFETs without and with PFOTES-coated TiO_2 nanoparticle protection layers before and after exposure to DI water (pH 6.7), HCl (pH 1.0), and NaOH (pH 13.0). Aforementioned, three representative organic semiconductors (evaporated pentacene, solution processed TIPS-pentacene, and P3HT) were chosen to demonstrate that the suggested superhydrophobic protection layer can be applied to a wide range of organic semiconductors, maintaining their electrical characteristics. The transfer (drain-source current versus gate voltage, I_{DS}–V_{GS}) characteristics were measured by sweeping V_{GS} from 40 to −60 V at a fixed drain-source voltage (V_{DS}) of −60 V (Figure 5a for pentacene OTFTs and Figure S25 for TIPS-pentacene and P3HT OFETs in the Supporting Information), and the output (drain-source current versus drain-source voltage, I_{DS}–V_{DS}) was measured by sweeping V_{DS} from 0 to −60 V at different V_{GS} from 0 to −60 V with an increment of −10 V (Figure 5b-d for pentacene OFETs and Figures S26 and S27 for TIPS-pentacene and P3HT OFETs, respectively, in the Supporting Information). To induce ordered crystals of organic semiconductors, surface treatment using a fluorinated solution was conducted on the SiO_2 dielectric layer, which provides a sufficient hydrophobic surface with a water-contact angle of 108°, and thus, the improved electrical performances were achieved (see Figure S28).[38] For the OFETs without the superhydrophobic protection layer, the unprotected devices exhibited a high I_{DS} value of over 10^{-5} A over the entire range of gate biases when exposed to water (Figures 5a,c and S29). Because extra current paths were created between the source-drain electrodes due to ionic conduction through the liquid on the bare active channel area, the current levels increased regardless of gate voltage. However, all of the protected OFETs showed no significant degradation of the electrical characteristics including a good current ratio (I_{on}/I_{off}) and field-effect mobility (μ_{FET}), even when they were exposed to various corrosive solutions (Figures 5a,d and S29 and Table S3). Even upon exposure to a tap water for 1000 s, we could not observe significant changes of the electrical characteristics (see Table S4 and Figure S30). Specifically, the carrier injection properties in the low-V_{DS} regime showed a good linearity without current degradation and were well-maintained during the solvent-robustness tests (see Figure S31). Furthermore, we performed the stability test measuring the electrical characteristics of the protected OFETs after storing them in a chamber with high humidity [75% relative humidity (RH) and 20 °C]. The threshold voltages (V_{TH}) of the unprotected OFETs evidently shifted by ~3.4 V on average toward the positive gate voltage direction as soon as they were exposed to high humidity, unlike the behavior of the protected devices showing no notable degradations (see Figures S32 and S33). After 5 days, the V_{TH} of the unprotected devices shifted by ~10 V, while the V_{TH} of the protected devices shifted only less than ~5 V, as shown in Figure 5e,f. It is well-known that this V_{TH} shift is attributed to water-molecules adsorption as previously reported.[39,40] More detailed information on the changes in electrical characteristics of OFETs with exposure to humid air are summarized in Table S5. Among metal oxide nanoparticle candidates, TiO_2 nanoparticle layers can also be a barrier against the adsorption with water-molecule because TiO_2 layers have shown a lower water vapor transmission rate (see Figure S34 and detailed information in section 3–7 of the Supporting Information).[41−43] In addition, PFOTES attached to the TiO_2 nanoparticles allows hydrophobicity to hinder the adsorption of water molecules.[44,45] However, there are grain boundaries between the PFOTES-coated TiO_2 nanoparticles that could act as paths for the interaction of water molecules with organic semiconductors. So, although the proposed protective layer could not prevent the permeability of moisture permanently, it could improve the environment-reliability against moisture especially in the early stage because its estimated water vapor transmission rate value was ~1.61 g m^{-2} day^{-1}, which was comparable with plastic packaging materials (see detailed information in section 3–8 of the Supporting Information).

CONCLUSIONS

In this study, the functionalized TiO_2 nanoparticle-based superhydrophobic protection layer was utilized to realize reliable OFETs. Because of the roughened surface and low surface energy of the protection layer, excellent water repellency and self-cleaning abilities were achieved, which could preserve the electrical characteristics of environmentally sensitive organic semiconductors. The suggested superhydrophobic protection layers were applied onto various organic semiconductors directly by a facile dipping process, exhibiting good resistances against mechanical, thermal, and light stress and chemical threats. In addition, they allowed more-reliable electrical characteristics of OFETs in ambient, even when exposed to strong solvents, due to its superhydrophobicity. This approach can be a good alternative solution for protecting low-cost and flexible organic electronics working in open air.

METHODS

Fabrication of Organic Field-Effect Transistors. The *p*-type heavily doped silicon substrates with 270 nm thick silicon dioxide (SiO_2) layers were sequentially cleaned with acetone, isopropanol, and DI water for 10 min each. On the cleaned substrate, Au/Ti (50 nm/5 nm) source and drain electrodes were deposited using an electron-beam evaporator with a deposition rate of 0.5 Å s^{-1} at a pressure of ~10^{-7} Torr. The surface treatment using a fluorinated

DOI: 10.1021/acsnano.8b05224
ACS Nano 2018, 12, 11062–11069

solution was conducted on the SiO_2 gate dielectric for the better organic semiconducting layer deposition. After UV−ozone treatment was done for 10 s to yield better wetting properties for the SiO_2 layer. Next, a PFOTES (0.5 g) solution dispersed in HFE-7200 (7 mL) was spin-coated with a spin speed of 500 rpm for 30 s, and unreacted residues of PFOTES were removed by rinsing with toluene. Samples were baked at 100 °C for 10 min on a hot plate. Then, a 120 nm thick pentacene active layer was thermally evaporated onto the sample surfaces that had patterned Au/Ti electrodes with a deposition rate of 0.2 Å s^{-1} at a pressure of ~10^{-5} Torr. The completed pentacene OFETs had a channel length and width of 60 and 300 μm, respectively. For TIPS-pentacene OFETs, 0.5 wt % TIPS-pentacene solution in toluene was drop-cast on the patterned Au/Ti source-drain electrodes with a channel length and width of 200 and 300 μm, respectively, and then the active layer was dried in air for 1 h. For P3HT OFETs, 1 wt % P3HT solution in 1,2-dichlorobenzene were spin-coated at 1500 rpm for 30 s onto the Au/Ti electrodes with a channel length and width of 100 and 300 μm, respectively, and then the sample was placed on a hot plate at 60 °C for 6 h in N_2.

Process of Superhydrophobic Protection Layer Formation. First, 8.0 g of TiO_2 nanoparticles (mixture of the rutile and anatase phases and nanoparticle diameter of <100 nm) and 0.5 g of PFOTES were placed into 29.8 mL of HFE-7500. The fabricated OFETs with three organic semiconductors were dipped into the HFE-7500 solution containing PFOTES and TiO_2 nanoparticles at room temperature for a short time (~2 s). The PFOTES-coated TiO_2 nanoparticles in the solution covered the surface of the OFETs. Finally, the OFETs with the superhydrophobic protection layer were dried with N_2 gas to remove any remaining solvent or residues.

Characterization. Cross-sectional images of the devices were obtained using scanning electron microscopy (MERLIN, ZEISS) and analytical scanning transmission electron microscopy (JEM-2100F, JEOL). To determine the surface moieties on the PFOTES-coated TiO_2 nanoparticle layers, XPS (Axis-HSI, Kratos Inc.) was conducted with an Al monochromator anode at a power of 18 mA and 12 kV. Roughness parameters were evaluated by using a 3D laser profiler (VK-250 K, KENENCE) and AFM (NX10, Park Systems Corp.). The contact angle, roll-off angle, and contact-angle hysteresis of the OFETs with and without the superhydrophobic protection layer were measured by standard procedures (SmartDrop Lab HS, Femtofab) in ambient conditions. The electrical characteristics of the fabricated OFETs were measured using a semiconductor parameter analyzer (model 4200 SCS, Keithley) and a probe station (model ST-500, JANIS).

ASSOCIATED CONTENT

Supporting Information

The Supporting Information is available free of charge on the ACS Publications website at DOI: 10.1021/acsnano.8b05224.

Details on the fabrication of OFETs with a superhydrophobic protection layer, superhydrophobic properties of PFOTES-coated TiO_2 nanoparticle layers, XPS spectra of PFOTES-uncoated TiO_2 nanoparticle layers, TEM images and EDS profiles of TIPS-pentacene and P3HT semiconducting layers with the PFOTES-coated TiO_2 nanoparticle layers, the durability of the organo-compatible superhydrophobic protection layer, electrical characteristics of protected and unprotected OFETs, and the water-vapor transmission rate of PFOTES-coated TiO_2 nanoparticle layers (PDF)

AUTHOR INFORMATION

Corresponding Authors

*E-mail: seungjun@kist.re.kr.
*E-mail: tlee@snu.ac.kr.

ORCID

Der-Hsien Lien: 0000-0001-6774-2074
Takhee Lee: 0000-0001-5988-5219

Present Address

[‖]Department of Materials Science and Engineering, University of North Texas, Texas 76207, United States

Notes

The authors declare no competing financial interest.

ACKNOWLEDGMENTS

This work was supported by the National Creative Research Laboratory Program (grant no. 2012026372) provided by the National Research Foundation of Korea (NRF). G.H.A., D.-H.L., and A.J. acknowledge the Electronic Materials Program, funded by the Director, Office of Science, Office of Basic Energy Sciences, Material Sciences and Engineering Division of the U.S. Department of Energy under contract no. DE-AC02-05CH11231. S.C. appreciates the support from the Korea Institute of Science and Technology (KIST) Future Resource Research Program (2E28310)

REFERENCES

(1) Forrest, S. R. The Path to Ubiquitous and Low-Cost Organic Electronic Appliances on Plastic. *Nature* **2004**, *428*, 911−918.
(2) Sekitani, T.; Yokota, T.; Zschieschang, U.; Klauk, H.; Bauer, S.; Takeuchi, K.; Takamiya, M.; Sakurai, T.; Someya, T. Organic Nonvolatile Memory Transistors for Flexible Sensor Arrays. *Science* **2009**, *326*, 1516−1519.
(3) Song, Y.; Jeong, H.; Jang, J.; Kim, T.-Y.; Yoo, D.; Kim, Y.; Jeong, H.; Lee, T. 1/f Noise Scaling Analysis in Unipolar-Type Organic Nanocomposite Resistive Memory. *ACS Nano* **2015**, *9*, 7697−7703.
(4) Zhou, Y.; Fuentes-Hernandez, C.; Shim, J.; Meyer, J.; Giordano, A. J.; Li, H.; Winget, P.; Papadopoulos, T.; Cheun, H.; Kim, J.; Fenoll, M.; Dindar, A.; Haske, W.; Najafabadi, E.; Khan, T. M.; Sojoudi, H.; Barlow, S.; Graham, S.; Brédas, J.-L.; Marder, S. R.; et al. A Universal Method to Produce Low-Work Function Electrodes for Organic Electronics. *Science* **2012**, *336*, 327−332.
(5) Sirringhaus, H. 25th Anniversary Article: Organic Field-Effect Transistors: The Path Beyond Amorphous Silicon. *Adv. Mater.* **2014**, *26*, 1319−1335.
(6) Klauk, H.; Zschieschang, U.; Pflaum, J.; Halik, M. Ultralow-Power Organic Complementary Circuits. *Nature* **2007**, *445*, 745−748.
(7) Diao, Y.; Tee, B. C-K.; Giri, G.; Xu, J.; Kim, D. H.; Becerril, H. A.; Stoltenberg, R. M.; Lee, T. H.; Xue, G.; Mannsfeld, S. C. B.; Bao, Z. Solution Coating of Large-Area Organic Semiconductor Thin Films with Aligned Single-Crystalline Domains. *Nat. Mater.* **2013**, *12*, 665−671.
(8) Baeg, K. J.; Caironi, M.; Noh, Y. Y. Solution Coating of Large-Area Organic Semiconductor Thin Films with Aligned Single-Crystalline Domains. *Adv. Mater.* **2013**, *25*, 4210−4244.
(9) Kang, H.; Kitsomboonloha, R.; Jang, J.; Subramanian, V. High-Performance Printed Transistors Realized Using Femtoliter Gravure-Printed Sub-10 μm Metallic Nanoparticle Patterns and Highly Uniform Polymer Dielectric and Semiconductor Layers. *Adv. Mater.* **2012**, *24*, 3065−3069.
(10) Chung, S.; Jang, M.; Ji, S. B.; Im, H.; Seong, N.; Ha, J.; Kwon, S.-K.; Kim, Y.-H.; Yang, H.; Hong, Y. Flexible High-Performance All-Inkjet-Printed Inverters: Organo-Compatible and Stable Interface Engineering. *Adv. Mater.* **2013**, *25*, 4773−4777.
(11) Sonar, P.; Singh, S. P.; Li, Y.; Soh, M. S.; Dodabalapur, A. A Low-Bandgap Diketopyrrolopyrrole-Benzothiadiazole-Based Copolymer for High-Mobility Ambipolar Organic Thin-Film Transistors. *Adv. Mater.* **2010**, *22*, 5409−5413.
(12) Sirringhaus, H. Reliability of Organic Field-Effect Transistors. *Adv. Mater.* **2009**, *21*, 3859−3873.

DOI: 10.1021/acsnano.8b05224
ACS Nano 2018, 12, 11062−11069

(13) Kaltenbrunner, M.; Sekitani, T.; Reeder, J.; Yokota, T.; Kuribara, K.; Tokuhara, T.; Drack, M.; Schwödiauer, R.; Graz, I.; Bauer-Gogonea, S.; Bauer, S.; Someya, T. An Ultra-Lightweight Design for Imperceptible Plastic Electronics. *Nature* **2013**, *499*, 458−463.
(14) McCulloch, I.; Heeney, M.; Bailey, C.; Genevicius, K.; MacDonald, I.; Shkunov, M.; Sparrowe, D.; Tierney, S.; Wagner, R.; Zhang, W.; Chabinyc, M. L.; Kline, R. J.; McGehee, M. D.; Toney, M. F. Liquid-Crystalline Semiconducting Polymers with High Charge-Carrier Mobility. *Nat. Mater.* **2006**, *5*, 328−333.
(15) Knopfmacher, O.; Hammock, M. L.; Appleton, A. L.; Schwartz, G.; Mei, J.; Lei, T.; Pei, J.; Bao, Z. Highly Stable Organic Polymer Field-Effect Transistor Sensor for Selective Detection in the Marine Environment. *Nat. Commun.* **2014**, *5*, 2954.
(16) Jinno, H.; Fukuda, K.; Xu, X.; Park, S.; Suzuki, Y.; Koizumi, M.; Yokota, T.; Osaka, I.; Takimiya, K.; Someya, T. Stretchable and Waterproof Elastomer-Coated Organic Photovoltaics for Washable Electronic Textile Applications. *Nat. Energy* **2017**, *2*, 780−785.
(17) Simon, D. T.; Kurup, S.; Larsson, K. C.; Hori, R.; Tybrandt, K.; Goiny, M.; Jager, E. W. H.; Berggren, M.; Canlon, B.; Richter-Dahlfors, A. Organic Electronics for Precise Delivery of Neurotransmitters to Modulate Mammalian Sensory Function. *Nat. Mater.* **2009**, *8*, 742−746.
(18) Sandström, A.; Dam, H.; Krebs, F.; Edman, L. Ambient Fabrication of Flexible and Large-Area Organic Light-Emitting Devices Using Slot-Die Coating. *Nat. Commun.* **2012**, *3*, 1002.
(19) Deng, X.; Mammen, L.; Zhao, Y.; Lellig, P.; Müllen, K.; Li, C.; Butt, H.-J.; Vollmer, D. Transparent, Thermally Stable and Mechanically Robust Superhydrophobic Surfaces Made from Porous Silica Capsules. *Adv. Mater.* **2011**, *23*, 2962−2965.
(20) Zakhidov, A. A.; Lee, J.-K.; Fong, H. H.; DeFranco, J. A.; Chatzichristidi, M.; Taylor, P. G.; Ober, C. K.; Malliaras, G. G. Hydrofluoroethers as Orthogonal Solvents for the Chemical Processing of Organic Electronic Materials. *Adv. Mater.* **2008**, *20*, 3481−3484.
(21) Wang, C.-Y.; Groenzin, H.; Shultz, M. J. Molecular Species on Nanoparticulate Anatase TiO_2 Film Detected by Sum Frequency Generation: Trace Hydrocarbons and Hydroxyl Groups. *Langmuir* **2003**, *19*, 7330−7334.
(22) Lu, Y.; Sathasivam, S.; Song, J.; Crick, C. R.; Carmalt, C. J.; Parkin, I. P. Robust Self-Cleaning Surfaces That Function When Exposed to Either Air or Oil. *Science* **2015**, *347*, 1132−1135.
(23) Lai, Y.; Tang, Y.; Gong, J.; Gong, D.; Chi, L.; Lin, C.; Chen, Z. Transparent Superhydrophobic/Superhydrophilic TiO_2-Based Coatings for Self-Cleaning and Anti-Fogging. *J. Mater. Chem.* **2012**, *22*, 7420−7426.
(24) Nishino, T.; Meguro, M.; Nakamae, K.; Matsushita, M.; Ueda, Y. The Lowest Surface Free Energy Based on -CF_3 Alignment. *Langmuir* **1999**, *15*, 4321−4323.
(25) Feng, L.; Li, S.; Li, Y.; Li, H.; Zhang, L.; Zhai, J.; Song, Y.; Liu, B.; Jiang, L.; Zhu, D. Super-Hydrophobic Surfaces: From natural to Artificial. *Adv. Mater.* **2002**, *14*, 1857−1860.
(26) Lafuma, A.; Quéré, D. Superhydrophobic States. *Nat. Mater.* **2003**, *2*, 457−460.
(27) Wang, S.; Jiang, L. Definition of Superhydrophobic States. *Adv. Mater.* **2007**, *19*, 3423−3424.
(28) Wang, P.; Zhao, T.; Bian, R.; Wang, G.; Liu, H. Robust Superhydrophobic Carbon Nanotube Film with Lotus Leaf Mimetic Multiscale Hierarchical Structures. *ACS Nano* **2017**, *11*, 12385−12391.
(29) Chen, S.; Li, X.; Li, Y.; Sun, J. Intumescent Flame-Retardant and Self-Healing Superhydrophobic Coatings on Cotton Fabric. *ACS Nano* **2015**, *9*, 4070−4076.
(30) Yuan, L.; Dai, J.; Fan, X.; Song, T.; Tao, Y. T.; Wang, K.; Xu, Z.; Zhang, J.; Bai, X.; Lu, P.; Chen, J.; Zhou, J.; Wang, Z. L. Self-Cleaning Flexible Infrared Nanosensor Based on Carbon Nanoparticles. *ACS Nano* **2011**, *5*, 4007−4013.
(31) Rioboo, R.; Voué, M.; Vaillant, A.; De Coninck, J. Drop Impact on Porous Superhydrophobic Polymer Surfaces. *Langmuir* **2008**, *24*, 14074−14077.
(32) Song, Z.; Hrbek, J.; Osgood, R. Formation of TiO_2 Nanoparticles by Reactive-Layer-Assisted Deposition and Characterization by XPS and STM. *Nano Lett.* **2005**, *5*, 1327−1332.
(33) Zhang, X.; Jiang, H.; Jin, J.; Xu, X.; Zhang, Q. Analysis of Acid Rain Patterns in Northeastern China Using a Decision Tree Method. *Atmos. Environ.* **2012**, *46*, 590−596.
(34) Shoenut, J. P.; Duerksen, D.; Yaffe, C. S. Impact of Ingested Liquids on 24-h Ambulatory pH Tests. *Dig. Dis. Sci.* **1998**, *43*, 834−839.
(35) Moreira, K. A.; Albuquerque, B. F.; Teixeira, M. F. S.; Porto, A. L. F.; Lima Filho, J. L. Application of Protease from Nocardiopsis sp. as a Laundry Detergent Additive. *World J. Microbiol. Biotechnol.* **2002**, *18*, 309−315.
(36) Ananthapadmanabhan, K. P.; Moore, D. J.; Subramanyan, K.; Misra, M.; Meyer, F. Cleansing Without Compromise: The Impact of Cleansers on the Skin Barrier and the Technology of Mild Cleansing. *Dermatol. Ther.* **2004**, *17*, 16−25.
(37) Nørgaard, A. W.; Jensen, K. A.; Janfelt, C.; Lauritsen, F. R.; Clausen, P. A.; Wolkoff, P. Release of VOCs and Particles During Use of Nanofilm Spray Products. *Environ. Sci. Technol.* **2009**, *43*, 7824−7830.
(38) Kim, S. H.; Jang, M.; Yang, H.; Anthony, J. E.; Park, C. E. Physicochemically Stable Polymer-Coupled Oxide Dielectrics for Multipurpose Organic Electronic Applications. *Adv. Funct. Mater.* **2011**, *21*, 2198−2207.
(39) Park, S. K.; Mourey, D. A.; Han, J. I.; Anthony, J. E.; Jackson, T. N. Environmental and Operational Stability of Solution-Processed 6, 13-Bis (triisopropyl-silylethynyl) Pentacene Thin Film Transistors. *Org. Electron.* **2009**, *10*, 486−490.
(40) Li, D.; Borkent, E. J.; Nortrup, R.; Moon, H.; Katz, H.; Bao, Z. Humidity Effect on Electrical Performance of Organic Thin-Film Transistors. *Appl. Phys. Lett.* **2005**, *86*, 042105.
(41) Seo, S. W.; Jung, E.; Lim, C.; Chae, H.; Cho, S. M. Moisture Permeation Through Ultrathin TiO_2 Films Grown by Atomic Layer Deposition. *Appl. Phys. Express* **2012**, *5*, 035701.
(42) Kim, L. H.; Jang, J. H.; Jeong, Y. J.; Kim, K.; Baek, Y.; Kwon, H.-J.; An, T. K.; Nam, S.; Kim, S. H.; Jang, J.; Park, C. E. Highly-Impermeable Al_2O_3/HfO_2 Moisture Barrier Films Grown by Low-Temperature Plasma-Enhanced Atomic Layer Deposition. *Org. Electron.* **2017**, *50*, 296−303.
(43) Kim, L. H.; Kim, K.; Park, S.; Jeong, Y. J.; Kim, H.; Chung, D. S.; Kim, S. H.; Park, C. E. Al_2O_3/TiO_2 Nanolaminate Thin Film Encapsulation for Organic Thin Film Transistors *via* Plasma-Enhanced Atomic Layer Deposition. *ACS Appl. Mater. Interfaces* **2014**, *6*, 6731−6738.
(44) Park, J. S.; Choi, W. Enhanced Remote Photocatalytic Oxidation on Surface-Fluorinated TiO_2. *Langmuir* **2004**, *20*, 11523−11527.
(45) Bekyarova, E.; Hanzawa, Y.; Kaneko, K.; Silvestre-Albero, J.; Sepulveda-Escribano, A.; Rodriguez-Reinoso, F.; Kasuya, D.; Yudasaka, M.; Iijima, S. Cluster-Mediated Filling of Water Vapor in Intratube and Interstitial Nanospaces of Single-Wall Carbon Nanohorns. *Chem. Phys. Lett.* **2002**, *366*, 463−468.

DOI: 10.1021/acsnano.8b05224
ACS Nano 2018, 12, 11062−11069